Published in final edited form as:
Langmuir. 2011 May 17; 27(10): 5976–5985. doi:10.1021/la2000415.

Enhancement of Surface Wettability via the Modification of Microtextured Titanium Implant Surfaces with Polyelectrolytes

Jung Hwa Park[†], **Zvi Schwartz**[‡], **Rene Olivares-Navarrete**[‡], **Barbara D. Boyan**[†,‡], and **Rina Tannenbaum**[*,†]

[†] Schools of Materials Science and Engineering, Georgia Institute of Technology, Atlanta, Georgia, United States

[‡] Biomedical Engineering, Georgia Institute of Technology, Atlanta, Georgia, United States

Abstract

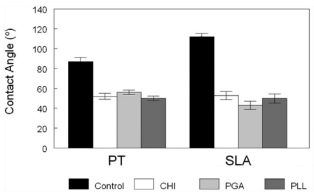

Micrometer- and submicrometer-scale surface roughness enhances osteoblast differentiation on titanium (Ti) substrates and increases bone-to-implant contact in vivo. However, the low surface wettability induced by surface roughness can retard initial interactions with the physiological environment. We examined chemical modifications of Ti surfaces [pretreated (PT), $R_a \geq 0.3$ μm; sand blasted/acid etched (SLA), $R_a \geq 3.0$ μm] in order to modify surface hydrophilicity. We designed coating layers of polyelectrolytes that did not alter the surface microstructure but increased surface ionic character, including chitosan (CHI), poly(L-glutamic acid) (PGA), and poly(L-lysine) (PLL). Ti disks were cleaned and sterilized. Surface chemical composition, roughness, wettability, and morphology of surfaces before and after polyelectrolyte coating were examined by X-ray photoelectron spectroscopy (XPS), contact mode profilometry, contact angle measurement, and scanning electron microscopy (SEM). High-resolution XPS spectra data validated the formation of polyelectrolyte layers on top of the Ti surface. The surface coverage of the polyelectrolyte adsorbed on Ti surfaces was evaluated with the pertinent SEM images and XPS peak intensity as a function of polyelectrolyte adsorption time on the Ti surface. PLL was coated in a uniform thin layer on the PT surface. CHI and PGA were coated evenly on PT, albeit in an incomplete monolayer. CHI, PGA, and PLL were coated on the SLA surface with complete coverage. The selected polyelectrolytes enhanced surface wettability without modifying surface roughness. These chemically modified surfaces on implant devices can contribute to the enhancement of osteoblast differentiation.

[*]**Corresponding Author**rinatan@mse.gatech.edu.

1. INTRODUCTION

The coating of surfaces with polyelectrolytes (PE) is a versatile approach to develop a robust and conformal surface through electrostatic forces.[1] A polyelectrolyte is a polymer whose repeating units possess an electrolyte group that will dissociate in aqueous solutions, such as water, to form polyions. Therefore, polyelectrolytes can consist of either positively charged groups (polycations) or negatively charged groups (polyanions) depending on the chemical nature of their repeating units and the pH of the aqueous solution.[1-3] Polyelectrolyte multilayers (PEMs) are formed by electrostatic interactions between the oppositely charged polyelectrolyte chains.[1,2,4] The structure of PEMs consists of three sections, as shown in Scheme 1. Section a is the first adsorbed layer on the substrate, section b is the bulk layer, and section c is the top layer, which is the dominant contributor to the chemical properties of the surface.[5]

The behavior of polyelectrolyte adsorption on a substrate is dependent upon charge density, polyelectrolyte molecular weight, pH, temperature, and ionic strength.[3,5-8] Consequently, these factors can affect polyelectrolyte diffusion or penetration among interlayers and control multilayer thickness.[9] In order to better understand PEMs, it is important to know the chemical polyelectrolyte, as shown in Scheme 1a, because the first adsorbed layer can directly affect the conformation and thickness of the next adsorbed polyelectrolyte layer.[10,11]

PEMs may be uniformly coated on substrates having a variety of sizes, shapes, and topographies, with high reproducibility.[1] Additionally, a polyelectrolyte-coated layer can also protect surfaces from corrosion, due to their pH-buffering properties. For example, coating of biomaterials, such as metal implants, with PEMs could increase the robustness and functional durability of such devices.[1,12,13] Because of these advantageous characteristics, the use of polyelectrolytes has emerged as a promising surface modification method, with potential applicability to the enhancement of the mechanical, chemical, and biocompatibility properties of biomedical devices. For example, chitosan (CHI) obtained by deacetylation of chitin has been shown to sustain osteoblast growth and inhibit the growth of fibroblasts.[14,15] Poly(L-glutamic acid) (PGA) and poly(L-lysine) (PLL) are synthetic poly(amino acid) polyelectrolytes, which exhibit positive and negative charges in solution, respectively. Substrates coated with PGA and PLL films are conducive to cell adhesion, depending on the pH of the medium.[16,17]

Titanium (Ti) is a well-known biomaterial for orthopaedic and dental implants. It has a high strength and fatigue resistance and a relatively low elastic modulus with low density compared to other metals.[18] The Ti surface has a very thin and stable oxide layer (average thickness 2–6 nm) on the surface that forms upon exposure to air or water, which in turn imparts biocompatibility and corrosion resistance properties to the material.[18-20] The Ti oxide layer consists mainly of TiO_2.[19] The isoelectric point (IEP) of TiO_2 is around pH 3.5–6.2.[21,22] It is altered as a function of solution pH, surface impurities, and crystal structure, including amorphous, anatase, and rutile.[18,23-25] TiO_2 has a negative charge in body fluids (pH 7.4), which is higher than the IEP range.

Previous studies have shown that Ti surface properties, such as surface roughness, surface energy, and surface chemistry, Influence bone formation.[26-28] Surface roughness on the micrometer scale can enhance osteoblast differentiation in vitro.[26,29-32] Microtextured Ti surfaces that are hydrophilic enhance tissue integration of titanium implants, especially during the early healing stages in vivo.[26,29,30,33–36] Surface chemistry also plays an important role in regulating the signaling pathways and downstream cell differentiation.[37,38] In order to reduce healing time and enhance osseointegration in compromised patients, it is important to understand, optimize, and engineer ideal surface properties for dental and orthopaedic implants used in bone applications.

The coating of polyelectrolytes, including CHI, PGA, or PLL, on various materials, such as silicon wafer, quartz, glass cover-slips, or TiO_2 particles, has been previously reported.[3,39-41] For example, Gao et al. described the coating of poly(L-lysine) and DNA on polished and alkali-treated titanium surfaces to build up multilayered films for understanding protein adsorption.[42] However, the adsorption of polyelectrolyte on the native oxide layer, which is spontaneously formed on a titanium surface, has seldom been probed. Moreover, micrometer-and submicrometer-scale rough Ti surfaces have not been directly coated with polyelectrolytes. Hence, in this paper, we developed a deposition process to form a thin polyelectrolyte film on the native titanium oxide layer on both pretreated (PT) and sand blasted/acid etched (SLA) Ti surfaces, similar to those used in clinical settings. Scheme 2 shows the polyelectrolytes used in this study. X-ray photoelectron spectroscopy (XPS), contact mode profilometry, contact angle measurements, and scanning electron microscopy (SEM) were used to characterize the chemical features of the polyelectrolyte-coated Ti surfaces to determine the surface chemistry, roughness, wettability, and surface coverage.

2. EXPERIMENTAL SECTION

2.1. Titanium Substrates

Ti disks were supplied by Institut Straumann AG (Basel, Switzerland) with 1 mm thickness and 15 mm diameter. The disks were manufactured to exhibit two different surface structures: a pretreated surface (PT, $R_a \leq 0.3\ \mu m$) and sand blasted/ acid-etched surface (SLA, $R_a \geq 3.0\ \mu m$).[30] Ti disks were cleaned with a sequential acetone–2-propanol-ethanol protocol, in which disks were rinsed twice for 15 min at each step. After cleaning, disks were rinsed with distilled water and sterilized with oxygen plasma followed by steam autoclave.

2.2. Preparation of Polyelectrolyte Solutions and Ti Surface Modification

Chitosan (CHI, M_w = 125 000–350 000 g/mol, deacetylation degree 80–89%, medical grade) was obtained from NovaMatrix (Drammen, Norway). Poly(L-glutamic acid) (PGA, M_w= 2000-15 000 g/mol) and poly(L-lysine) (PLL, M_w = 150 000–300 000 g/mol, medical grade) were purchased from Sigma-Aldrich (St. Louis, MO). Glacial acetic acid, sodium chloride, acetone, 2-propanol, and ethanol were obtained from Sigma-Aldrich. PGA and PLL solutions consisted of 0.1 mg/mL in 0.15 M aqueous NaCl. The CHI solution consisted of 1.5 mg/mL dissolved in 0.1 M acetic acid containing 0.14 M aqueous NaCl.[14] All

polyelectrolyte solutions were filtered through a sterilized poly(tetrafluoroethylene) (PTFE) filter (pore size 0.2 μm) before exposure to the surface. The polyelectrolyte layer (PEL) was prepared on the cleaned and sterilized PT and SLA surfaces by immersing the substrates in 300 μL of the polyelectrolyte solutions at room temperature for 2 h. Each coating was followed by a 5 min rinse in either 0.15 M NaCl for PGA and PLL coatings or 0.14 M NaCl for CHI. Surfaces were allowed to dry under a UV sterilized hood after the final coating. The filtering and coating processes were performed in a UV-sterilized hood. Polyelectrolyte-coated surfaces are denoted as substrate-polyelectrolyte. For example, PT-CHI represents PT surface coated with chitosan (CHI).

2.3. Surface Characterization

X-ray photoelectron spectroscopy (XPS) measurements were performed on an ESCA-SSX 100 (Service Physics, Bend, OR) instrument equipped with a monochromatic Al KR X-ray source ($h\nu$ = 1486.6 eV). The XPS analysis chamber was evacuated to a pressure of 10^{-8} Torr or lower before collecting XPS spectra. High-resolution spectra were obtained using an X-ray spot size of 200 μm and pass energy of 50 eV, with a 0.1 eV increment, at a 55° takeoff angle. Peak fitting was performed using symmetric curves that were 80% Gaussian and 20% Lorentzian. Evaluation of XPS results was carried out using the ESCA 2005G software package provided by Service Physics, Inc.

The surface roughness before and after coating was measured two-dimensionally with a KLA-Tencor P-15 contact mode profilometer (KLA Tencor, CA) equipped with a 2 μm diamond-tracing stylus tip and a 90° point angle. Six random areas were measured on each sample over a scan length of 500 μm to obtain an average roughness value (R_a, μm).

Contact angle measurement using doubly distilled water was conducted by using a CAM 100 goniometer (KSV Instruments Ltd.) before and after coating. Image analysis was performed by using the KSV CAM 100 software package provided by KSV. Six samples were measured in each group, and two measurements were made from each surface. Polyelectrolyte-coated PT and SLA surface morphology as a function of adsorption time was examined by scanning electron microscopy (SEM) using an Ultra 60 field emission (FE) microscope (Carl Zeiss SMT Ltd., Cambridge, UK). Samples were coated with gold, and images were recorded using a 5 kV accelerating voltage.

2.4. Statistical Analysis

The data given are the mean (standard error of six individual surfaces for contact angle and profilometry. Data were first analyzed by analysis of variance (ANOVA). When differences were detected, a Student's *t*-test for multiple comparisons using Bonferroni's modification was used. The $p < 0.05$ was considered to be significant.

3. RESULTS AND DISCUSSION

3.1. XPS Chemical Analysis of Polyelectrolyte Layer

To ascertain the adsorption of polyelectrolytes on the PT and SLA surfaces, XPS analysis was conducted before and after polyelectrolyte coating. Figure 1 shows the Ti(2p) high-

resolution XPS spectra of both metallic Ti and TiO_2 on the bare samples and on samples having the adsorbed polyelectrolyte films. Prior to the polyelectrolyte deposition, both species are detectable on the surface. The presence of the Ti($2p_{3/2}$) and Ti($2p_{½}$) peaks of TiO_2 at 458.20 and 464.88 eV, respectively, observed in the spectra of the coated substrates, suggests that the adsorbed polyelectrolytes formed a thin film on the PT or SLA surfaces, having a thickness that was smaller than the penetration depth of the X-ray in the sample (~7 nm).[42] Unlike the TiO_2 peaks, the small $Ti^{(0)}$ peak at 454.34 eV is visible only in the PT-CHI and PT-PGA samples (Figure 1a), and absent in the PT-PLL and all the coated SLA samples (Figure 1b). This suggests that in the PT-CHI and PT-PGA samples there is only partial polyelectrolyte coverage, while in the PT-PLL, SLA-CHI, SLA-PGA, and SLA-PLL samples the coverage is more extensive. This information was further corroborated by the results from SEM images as shown in Figures 4 and 5.

Figure 2 shows the XPS high resolution analysis of the C(1s), O(1s), and N(1s) core level electrons for the PT control, PTCHI, PT-PGA, and PT-PLL surfaces. The PT control surface has three elements: titanium (Ti), oxygen (O), and carbon (C). Ti and oxygen originate from the native TiO_2 layer on the surface as shown in Figure 1.[19] The carbon is most likely a result of carbon-containing molecules due to exposure to the ambient environment.[20] Lausmaa et al. pointed out that the Ti surface always displayed Ti, O, C, and N peaks by XPS general survey.[19] However, an N signal was not detected on PT surfaces used in this study. The C(1s) XPS spectrum of the PT control surface (Figure 2a) shows the aliphatic carbon peak at 284.74 eV and additional peaks at 286.17 and 288.0 eV, corresponding to a C–O single bond and C=O double bond, respectively. The amine (C-N) peak was not detected on the PT control surface (Figure 2a). However, after adsorption of CHI (Figure 2d), PGA (Figure 2g), and PLL (Figure 2j) to the PT surface, the C(1s) XPS spectra indicated the presence of amine (C-N) bands at 286.45, 285.66, and 286.23 eV, respectively.

There is a significant carboxylate ($–COO^-$) peak at 288.42 eV on the PT-PGA surface (Figure 2g). It is interesting to note that the titanium oxide layer is weakly negatively charged, and PGA has the same charge as the titanium oxide layer. If the electrostatic force is the only source of the interaction between the Ti surface and PGA, there is a quite limited way to adsorb PGA on the Ti surface. However, XPS, considered one of the most surface sensitive analyses, detected the carboxylate ($–COO^-$) peak on the Ti surface following the adsorption of the PGA, a fact that is commensurate with PGA presence on the surface. Therefore, XPS high resolution analysis data suggest a possible chemical interaction between the oxide layer and PGA, rather than just an electrostatic interaction.[17,40,43] Also, the negatively charged PGA in solution can be screened due to the repellent force induced by like-charge with the Ti surface. Thus Na^+ ions can have more interaction with a negatively charged Ti surface. Therefore, an electrical double layer may be formed on the Ti surface, causing a limited charge inversion in the double layer, thereby leading to the adsorption of PGA.[8,44,45]

High-resolution XPS spectra of the O(1s) core electrons of the PT control surface (Figure 2b) show three components: a titanium oxide peak at 530.10 eV, a carbon–oxygen double bond (CdO) at 531.59 eV, and a hydroxide bond (C–OH) at 532.50 eV. The O(1s) peak shapes are changed after coating with CHI, PGA, and PLL on PT surface corresponding to

parts e, h, and k of Figure 2, respectively. The PT-PGA surface (Figure 2h) and PTPLL surface (Figure 2k) show similar overall spectral contour in the O(1s) binding energy region because they are both synthetic amino acids, as shown in Scheme 2. The peak at 532.09 eV on the PT-PGA surface (Figure 2h) belongs to the COO^- group. This carboxylate peak clearly shows that PGA is adsorbed on the PT surface. The different spectral contours of the high-resolution peaks among control and modified surfaces can be used as a good index to confirm polyelectrolyte adsorption on the PT surface. The XPS spectral contour is a result of the population density of the specific chemical species on the surfaces.[46]

The N(1s) core bands for the PT control surface (Figure 2c) were not detected. However, PT-CHI (Figure 2f), PT-PGA (Figure 2i), and PT-PLL (Figure 2l) surfaces showed N(1s) core bands of the carbon-nitrogen (C-N) group at 399.85, 400.18 and 399.98 eV, respectively. The adsorption of CHI, PGA, and PLL on PT surfaces affect the shape of the N(1s) peak. This N(1s) peak results from the amino and amide groups that are present in three polyelectrolytes used in this study, as shown in Scheme 2. In addition, charged nitrogen (NH_3^+) was detected in the N(1s) core spectra at 402.41 eV on PT-CHI surfaces (Figure 2f) and 401.99 eV on PT-PLL surfaces (Figure 2l), which is in good agreement with the other reported peaks for charged nitrogen species.[47,48] The high-resolution XPS analysis of the control and modified PT surfaces, particularly the presence of the carboxylate group on the PT-PGA surface and the nitrogen-containing functional groups on the PT-CHI surface and the PT-PLL surface, confirm that CHI, PGA, and PLL were adsorbed onto the PT surfaces.

High-resolution XPS spectra of C(1s), O(1s), and N(1s) electrons for the SLA control and the polyelectrolyte coated surfaces, as shown in Figure 3, were obtained in a similar manner as those described for the PT surfaces. In contrast to the PT control surface (Figure 2c), the N(1s) peak was detected on the SLA control surface (Figure 3c). PT and SLA surfaces were extensively cleaned and sterilized before coating, and therefore, there is a small probability that small molecules could be trapped on the surface. One possible explanation for the observation of the N(1s) peak on the SLA control (Figure 3c) is the presence of a small detectable amount of impurity, such as nitride (TiN), on the oxide surface.[19] Also, this discrepancy between PT and SLA surfaces may be due to the difierence in surface roughness between the comparatively smooth PT surface and the complex morphology of the rough SLA surface, both at the micrometer and submicrometer size scales. Therefore, the N(1s) signal cannot be fully accepted as validation of the adsorption of polyelectrolytes on the SLA surface. Therefore, following the systematic deconvolution of the high-resolution N(1s) spectral contour, the percent total area specifically of the C–N peak is used to demonstrate the presence of the polyelectrolyte coating on the SLA surfaces. The high-resolution N(1s) spectral contour was different among the various samples, corresponding to the variations in the chemical composition of the polyelectrolytes, leading to different percent total areas for each surface. The percent total area of the C-Npeakfor SLA-CHI (61%), SLA-PGA (73%), and SLA-PLL (63%) was higher than that for the SLA control (29%) surface. The increase in the intensity of the C–N peak following CHI, PGA, and PLL deposition suggests that the polyelectrolytes were indeed adsorbed on the SLA surface. Moreover, charged nitrogen (NH_3^+)peaks at 402.83 and 402.09 eV were observed on the SLA-CHI surface (Figure 3f) and the SLA-PLL surface (Figure 3l), respectively. The

carboxylate ($–COO^–$) peak at 532.05 eV on the SLA-PGA surface (Figure 3h) confirmed the presence of the PGA on the modified SLA surface. XPS analysis demonstrated the adsorption of CHI, PGA, and PLL polyelectrolytes on the SLA surface.

3.2. Polyelectrolyte Surface Coverage on Ti Surfaces

The surface coverage defined by the number of adsorbed molecules per unit surface area is important for understanding the interactions between the Ti surface and the polyelectrolytes. Since both the PT and SLA samples have rough surfaces (albeit different degrees of roughness), it is a challenge to measure accurate surface area for the calculation of surface coverage. Therefore, the surface coverage of the polyelectrolytes adsorbed on Ti surfaces was evaluated by examining the pertinent SEM images of the covered surfaces, which are shown in Figures 4 and 5, and supported by a quantitative XPS analysis. The PT and SLA surfaces coated with CHI, PGA, and PLL do not exhibit any noteworthy morphological changes when compared to controls under low magnification. However, under high magnification, it appears that the CHI (Figure 4d) and PGA (Figure 4f) poly-electrolytes coated the Ti substrates evenly, albeit in an incomplete layer.

The flexibility of the polyelectrolyte chain, i.e., the balance between chain conformation and chain affinity for the surface, determines its ability to adsorb onto the surface, and hence, it plays an important role in determining the amount of adsorbed polyelectrolyte on substrates.[44,49] Since CHI has abundant hydroxide groups that can form H-bonds between chains, the polymer acts as a rigid and stiff network,[50] causing conformational and entropic barriers to adsorption. The PT-PGA system (Figure 4f) shows similar surface morphology to that of the PTCHI system. PGA cannot efficiently adsorb on Ti surfaces due to the repulsive force generated by the same charges found on both materials. However, XPS, contact angle, and SEM images have shown conclusively that PGA has indeed adsorbed on the Ti surface.

Like-charge polyelectrolyte interactions can be explained by the competition among the negatively charged titanium oxide surface, PGA ($–COO^–$), and Na^+ ions, which originate from the 0.15 M NaCl salt solution used in this study. The Na^+ ions in solution are attracted to and interact with the negatively charged titanium oxide surface, thereby reducing the negative character of the surface and allowing the PGA to adsorb.

The PT-PLL (Figure 4h) shows uniform coverage on the entire surface. It is dificult to differentiate between the surface morphology of the control and that of the PLL coated surfaces, even under high magnification, indicating that PLL is coated on the PT surface without any change in surface morphology. The inset in Figure 4h also shows that when a small portion of the PLL overlayer is torn off, the underlying dark PT surface is exposed. This highlights the uniformity of the polyelectrolyte thin layer formed on the surface.

Polyelectrolyte-modified SLA surfaces exhibit different surface morphology than that obtained for PT surfaces, as shown in Figure 5. In addition to the adsorbed polyelectrolytes, small salt crystals were also observed on the modified SLA surfaces, most likely generated when rinsing with the NaCl solution. PT and SLA are commercially pure Ti, and the discrepancy between PT and SLA surfaces is their inherent different surface morphology. The SLA surface has micrometer and submicrometer scale roughness. It is possible that the

surface morphology affects polyelectrolyte adsorption. Nunnery et al. showed that the surface curvature can affect the polymer adsorption behavior and consequently the coverage of the polymer on surfaces.[51] Because the SLA surface morphology can be described as concave on the micrometer scale (hence, at least 2 orders of magnitude larger than the effective R_g of the polymers), there is no direct and strong effect on polyelectrolyte chain adsorption. However, the curvature of the SLA surface caused by the higher degree of surface roughness can contribute to an increase of the surface area. The adsorption mechanism of polyelectrolytes on surfaces with complex surface morphologies at both the micrometer-and nanoscale is not clear.

The incomplete coverage of CHI on PT, after the standard 2 h incubation time used for all the samples, was contrary to our expectations, given the positive ionic charge of the polymer. To better assess whether the incomplete coverage was thermodynamically mandated or a result of insuficient adsorption time, we probed the adsorption behavior of the CHI layer on PT and the resulting surface properties as a function of time, as shown in Figure 6. The extent of coverage of the adsorbed CHI on PT surfaces was monitored by XPS. The atomic abundance of Ti and N, expressed as atom %, was plotted as a function of the adsorption time (Figure 6a). When the angle of incidence of the X-ray beam is fixed, the amount of Ti and N detected depends on the distance of the species from the surface and hence it will change as a function of the polymer layer thickness. The initial decrease of the Ti atom % and the increase of the N atom % are due to the increased polymer coverage. This is coupled with a moderate increase in the coating layer roughness immediately following the onset of adsorption (Figure 6b) and a decrease in the coating layer contact angle (Figure 6c). After approximately 24 h of adsorption time, the Ti peak was barely detectable by XPS, suggesting that the whole PT surface was covered with CHI. Moreover, after this amount of time, both surface roughness and contact angle reached a constant value, indicating the formation of a complete monolayer.

3.3. Surface Roughness

The surface roughness of the polyelectrolyte-modified surface was measured with contact mode profilometry before and after the adsorption of the polyelectrolytes on both the PT and SLA surface. Figure 7a shows that surface roughness (R_a, μm) was not significantly altered after coating of the PT and SLA surfaces. Surface roughness has been recognized as one of the most important surface properties in osteoblast differentiation on Ti substrates and in bone-to-implant contact in vivo and in vitro.[16,35] The modification of the chemical properties of the Ti surfaces while preserving their surface roughness could represent an attractive option for the enhancement of their properties and the cell response.

3.4. Surface Wettability

Both surface roughness and surface chemistry can directly influence surface wettability.[52,53] In turn, surface wettability can be ascertained by the measurement of water contact angles (surface hydrophylicity).[54-56] Since both PT and SLA are made of commercially pure Ti, the difference in contact angle between them is due to their different surface treatments, which resulted in a rougher surface for SLA. As a result, the SLA control surface is more hydrophobic than the PT control surface, as exhibited by its larger contact angle, shown in

Figure 7b. The wettabilities of the PT and SLA control surfaces were significantly enhanced when their native oxide layers were coated with CHI, PGA, and PLL, as evidenced by a decrease in the measured contact angles, as shown in Figure 7b. There was no statistical difference in contact angles among modified PT and SLA surfaces. While the higher roughness of the uncoated SLA sample implied the availability of a larger surface, and hence, a larger amount of polyelectrolyte chains that could potentially adsorb, the fact that the surface roughness was not altered indicated that both coated substrates had similar charge densities. Therefore, the changes in surface hydrophylicity and, in particular ,the drastic change observed for SLA must be due to the nature of the polyelectrolyte coating itself. These results clearly show that we were able to decouple the effects of surface roughness and surface chemistry on surface wettability. Furthermore, we have shown that surface chemistry is the dominant parameter governing surface properties, with the underlying microtexture playing only a secondary role.

4. CONCLUSIONS

We have developed a facile method for the surface modification of Ti surfaces by the adsorption of three different polyelectrolytes: CHI, PGA, and PLL. The coated Ti surfaces were characterized by a variety of methods to ascertain the adsorption of the polyelectrolytes and to evaluate their Influence on the surface properties of the Ti surfaces. The results show that the polyelectrolytes used in this study were successfully adsorbed onto PT and SLA surfaces and enhanced surface wettability without modifying the surface roughness of the substrates. Surprisingly, there was no statistical difference in contact angles among all coated PT and SLA surfaces, with the SLA substrate sustaining a more pronounced decrease than that of PT. The fact that the surface roughness of the substrates was not altered upon polymer adsorption indicated that both coated substrates had similar charge densities. Therefore, the nature of the polyelectrolyte coating itself must have been responsible for the changes in surface hydrophylicity. These results clearly show that we were able to decouple the effects of surface roughness and surface chemistry on surface wettability. Furthermore, we have shown that, in these systems, surface chemistry is the dominant parameter governing surface properties, with the underlying micro-texture playing only a secondary role.

Surface roughness and wettability have been shown to improve wound healing and osseointegration process. Our results suggest that polyelectrolyte surface modification on Ti surfaces, a process which can be achieved without roughness modification, could enhance bone formation and increase osseointegration in dental and orthopedic implants.

ACKNOWLEDGMENT

This work was supported by an USPHS Grant AR052102 and the ITI Foundation. A graduate fellowship (to J.H.P.) was awarded by the Paper Science and Engineering (PSE) program and funded through the Institute of Paper Science and Technology (IPST) at Georgia Tech. The PT and SLA disks were provided by Institut Straumann AG.

REFERENCES

(1). Decher G. Science. 1997; 277:1232.
(2). Hammond PT. Adv. Mater. 2004; 16:1271.

(3). Yoo D, Shiratori SS, Rubner MF. Macromolecules. 1998; 31:4309.
(4). Tang ZY, Wang Y, Podsiadlo P, Kotov NA. Adv. Mater. 2006; 18:3203.
(5). Ladam G, Schaad P, Voegel JC, Schaaf P, Decher G, Cuisinier F. Langmuir. 2000; 16:1249.
(6). Clark SL, Montague MF, Hammond PT. Macromolecules. 1997; 30:7237.
(7). McAloney RA, Sinyor M, Dudnik V, Goh MC. Langmuir. 2001; 17:6655.
(8). Dan N. Nano Lett. 2003; 3:823.
(9). Halthur TJ, Elofsson UM. Langmuir. 2004; 20:1739. [PubMed: 15801437]
(10). de Gennes PG. Adv. Colloid Interface. 1987; 27:189.
(11). Castelnovo M, Joanny JF. Langmuir. 2000; 16:7524.
(12). Andreeva DV, Fix D, Mohwald H, Shchukin DG. J. Mater. Chem. 2008; 18:1738.
(13). Laurent D, Schlenoff JB. Langmuir. 1997; 13:1552.
(14). Chua PH, Neoh KG, Kang ET, Wang W. Biomaterials. 2008; 29:1412. [PubMed: 18190959]
(15). Lahiji A, Sohrabi A, Hungerford DS, Frondoza CG. J. Biomed. Mater. Res. 2000; 51:586. [PubMed: 10880106]
(16). Richert L, Arntz Y, Schaaf P, Voegel JC, Picart C. Surf. Sci. 2004; 570:13.
(17). Schmidt M. Arch. Orthopaed. Trauma Surg. 2001; 121:403.
(18). Tengvall P, Lundstrom I. Clin. Mater. 1992; 9:115. [PubMed: 10171197]
(19). Lausmaa J, Kasemo B, Mattsson H. Appl. Surf. Sci. 1990; 44:133.
(20). Lausmaa J. J. Electron Spectrosc. 1996; 81:343.
(21). Roessler S, Zimmermann R, Scharnweber D, Werner C, Worch H. Colloid. Surf. B. 2002; 26:387.
(22). Parks GA. Chem. Rev. 1965; 65:177.
(23). Foissy A, Mpandou A, Lamarche JM, Jaffrezicrenault N. Colloids Surf. 1982; 5:363.
(24). Kosmulski M, Gustafsson J, Rosenholm JB. Colloid Polym. Sci. 1999; 277:550.
(25). Sugita M, Tsuji M, Abe MB. Chem. Soc. Jpn. 1990; 63:559.
(26). Zhao G, Raines AL, Wieland M, Schwartz Z, Boyan BD. Biomaterials. 2007; 28:2821. [PubMed: 17368532]
(27). Schwartz Z, Boyan BD. J. Cell. Biochem. 1994; 56:340. [PubMed: 7876327]
(28). Boyan BD, Hummert TW, Dean DD, Schwartz Z. Biomaterials. 1996; 17:137. [PubMed: 8624390]
(29). Schwarz F, Wieland M, Schwartz Z, Zhao G, Rupp F, Geis-Gerstorfer J, Schedle A, Broggini N, Bornstein MM, Buser D, Ferguson SJ, Becker J, Boyan BD, Cochran DL. J. Biomed. Mater. Res. B. 2009; 88B:544.
(30). Rupp F, Scheideler L, Olshanska N, de Wild M, Wieland M, Geis-Gerstorfer J. J. Biomed. Mater. Res. A. 2006; 76A:323. [PubMed: 16270344]
(31). Kieswetter K, Schwartz Z, Hummert TW, Cochran DL, Simpson J, Dean DD, Boyan BD. J. Biomed. Mater. Res. 1996; 32:55. [PubMed: 8864873]
(32). Olivares-Navarrete R, Raz P, Zhao G, Chen J, Wieland M, Cochran DL, Chaudhri RA, Ornoy A, Boyan BD, Schwartz Z. Proc. Natl. Acad. Sci. U. S. A. 2008; 105:15767. [PubMed: 18843104]
(33). Molenberg A, Schwarz F, Herten M, Berner S, de Wild M, Wieland M. Materialwiss. Werkst. 2009; 40:31.
(34). Elias CN, Oshida Y, Lima JHC, Muller CA. J. Mech. Behav. Biomed. 2008; 1:234.
(35). Yahyapour N, Eriksson C, Malmberg P, Nygren H. Biomaterials. 2004; 25:3171. [PubMed: 14980412]
(36). Zhao G, Schwartz Z, Wieland M, Rupp F, Geis-Gerstorfer J, Cochran DL, Boyan BD. J. Biomed. Mater. Res. A. 2005; 74A:49. [PubMed: 15924300]
(37). Keselowsky BG, Collard DM, Garcia AJ. Proc. Natl. Acad. Sci. U. S. A. 2005; 102:5953. [PubMed: 15827122]
(38). Zreiqat H, Valenzuela SM, Ben Nissan B, Roest R, Knabe C, Radlanski RJ, Renz H, Evans PJ. Biomaterials. 2005; 26:7579. [PubMed: 16002135]

(39). Dierich A, Le Guen E, Messaddeq N, Stoltz JF, Netter P, Schaaf P, Voegel JC, Benkirane-Jessel N. Adv. Mater. 2007; 19:693.

(40). Markarian MZ, Moussallem MD, Jomaa HW, Schlenoff JB. Biomacromolecules. 2007; 8:59. [PubMed: 17206788]

(41). Tentorio A, Canova L. Colloids Surf. 1989; 39:311.

(42). Gao WL, Feng B, Ni YX, Yang YL, Lu XO, Weng J. Appl. Surf. Sci. 2010; 257:538.

(43). Roiter Y, Minko S. J. Phys. Chem. B. 2007; 111:8597. [PubMed: 17555343]

(44). Ouz EC, Messina R, Löwen H. J. Phys.:Condens. Matter. 2009; 21:464114. [PubMed: 21715878]

(45). Messina R, Holm C, Kremer K. J. Chem. Phys. 2002; 117:2947.

(46). Jedlicka SS, Rickus JL, Zemyanov DY. J. Phys. Chem. B. 2007; 111:11850. [PubMed: 17880200]

(47). Rojas OJ, Ernstsson M, Neumann RD, Claesson PM. J. Phys. Chem. B. 2000; 104:10032.

(48). Martin HJ, Schulz KH, Bumgardner JD, Walters KB. Langmuir. 2007; 23:6645. [PubMed: 17488131]

(49). Wallin T, Linse P. Langmuir. 1996; 12:305.

(50). Brugnerotto J, Desbrieres J, Roberts G, Rinaudo M. Polymer. 2001; 42:9921.

(51). Nunnery G, Hershkovits E, Tannenbaum A, Tannenbaum R. Langmuir. 2009; 25:9157. [PubMed: 19415910]

(52). Koch K, Barthlott W. Philos. Trans. R. Soc. A. 2009; 367:1487.

(53). Gao LC, McCarthy TJ. Langmuir. 2007; 23:3762. [PubMed: 17315893]

(54). Yoshimitsu Z, Nakajima A, Watanabe T, Hashimoto K. Langmuir. 2002; 18(15):5818.

(55). Feng L, Li S, Li Y, Li H, Zhang L, Zhai J, Song Y, Liu B, Jiang L, Zhu D. Adv. Mater. 2002; 14(24):1857.

(56). Sbragaglia M, Benzi R, Biferale L, Succi S, Toschi F. Phys. Rev. Lett. 2006; 97:204503. [PubMed: 17155685]

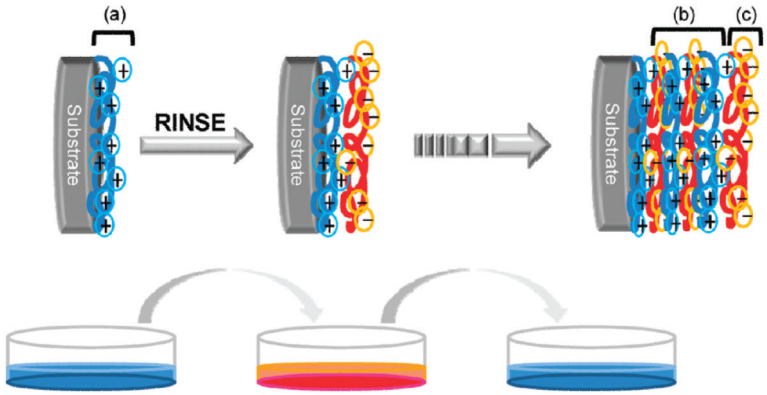

Scheme 1. Representation of the Deposition of the Alternating Polyelectrolyte Layers on Charged Substrate[a]

[a] Section a is the first adsorbed layer on the substrate, section b is the bulk layers encased between the first layer and the outermost layer, and section c is the top layer.

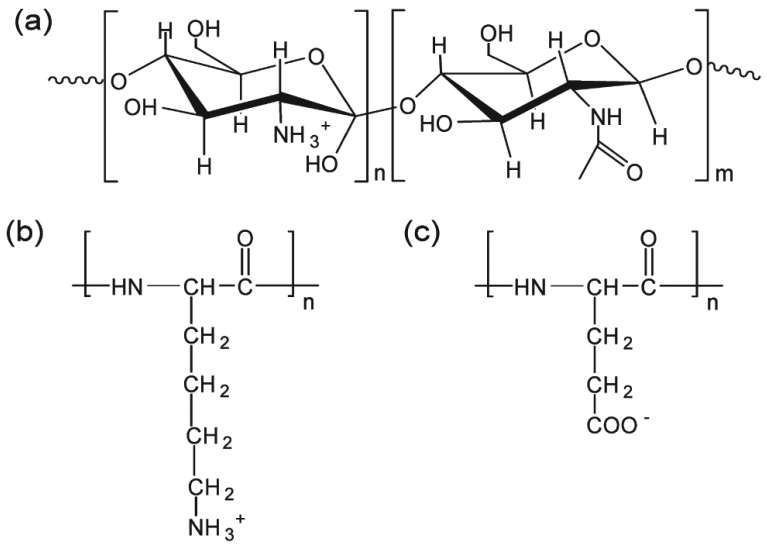

Scheme 2.

Chemical Structure of the Polyelectrolytes Used for the Surface Modification of Titanium Implant Surface: (a) Chitosan (CHI), (b) Poly(L-lysine) (PLL), and (c) Poly(Lglutamic acid) (PGA)

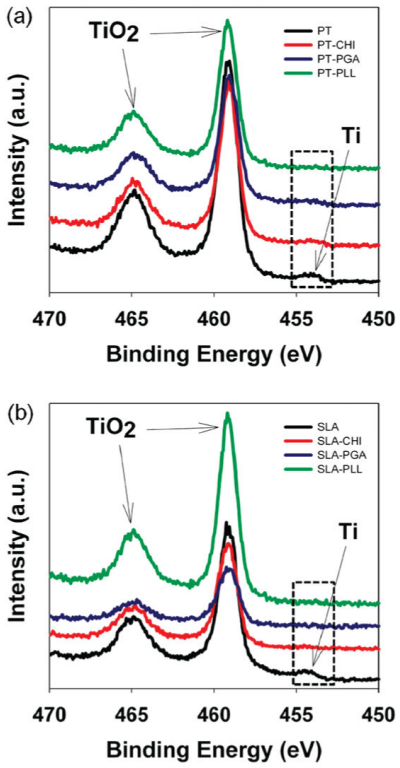

Figure 1.

X-ray photoelectron spectroscopy (XPS) spectra analysis. Evolution of Ti(2p) of Ti surfaces before and after polyelectrolyte coating: (a) PT and PT-polyelectrolyte and (b) SLA and SLA-polyelectrolyte surfaces.

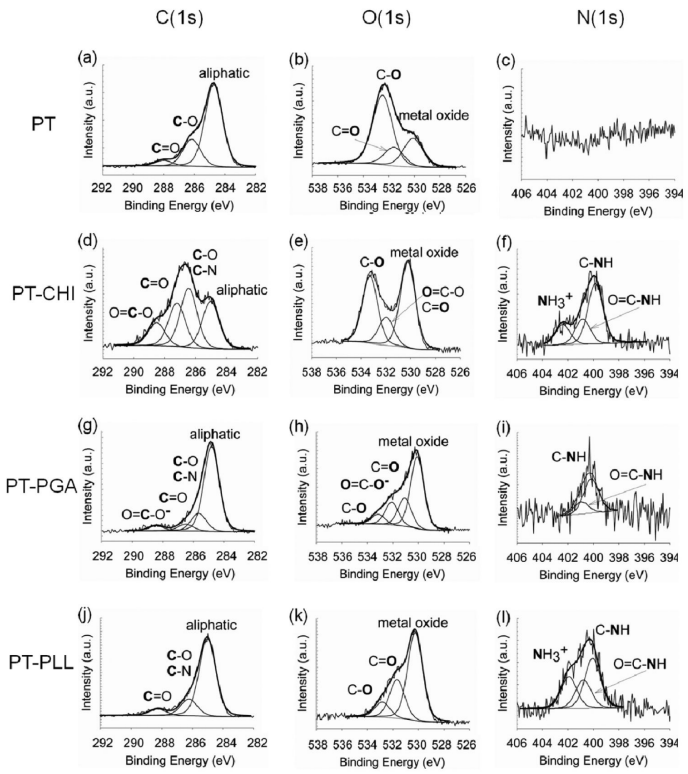

Figure 2.

High-resolution X-ray photoelectron spectroscopy (XPS) spectra of PT surfaces before and after polyelectrolyte coating: a, b, and c correspond to the C(1s), O(1s), and N(1s) core electrons of the control PT, respectively; d, e, and f correspond to the C(1s), O(1s), and N(1s) core electrons of the PT coated with chitosan (CHI), respectively; g, h, and i correspond to the C(1s), O(1s), and N(1s) core electrons of the PT coated with poly(L-glutamic acid), respectively; and j, k, and l correspond to the C(1s), O(1s), and N(1s) core electrons of the PT coated with poly(L-lysine), respectively.

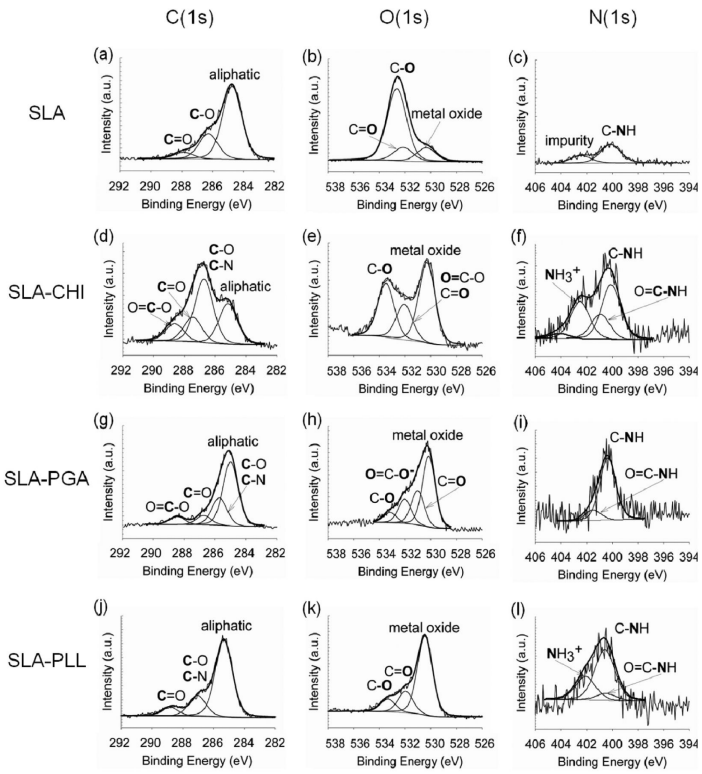

Figure 3.

High resolution X-ray photoelectron spectroscopy (XPS) spectra of SLA surfaces before and after polyelectrolyte coating: a, b, and c correspond to the C(1s), O(1s), and N(1s) core electrons of the control SLA, respectively; d, e, and f correspond to the C(1s), O(1s), and N(1s) core electrons of the SLA coated with chitosan (CHI), respectively; g, h, and i correspond to the C(1s), O(1s), and N(1s) core electrons of the SLA coated with poly(L-glutamic acid), respectively; and j, k, and l correspond to the C(1s), O(1s), and N(1s) core electrons of the SLA coated with poly(L-lysine), respectively.

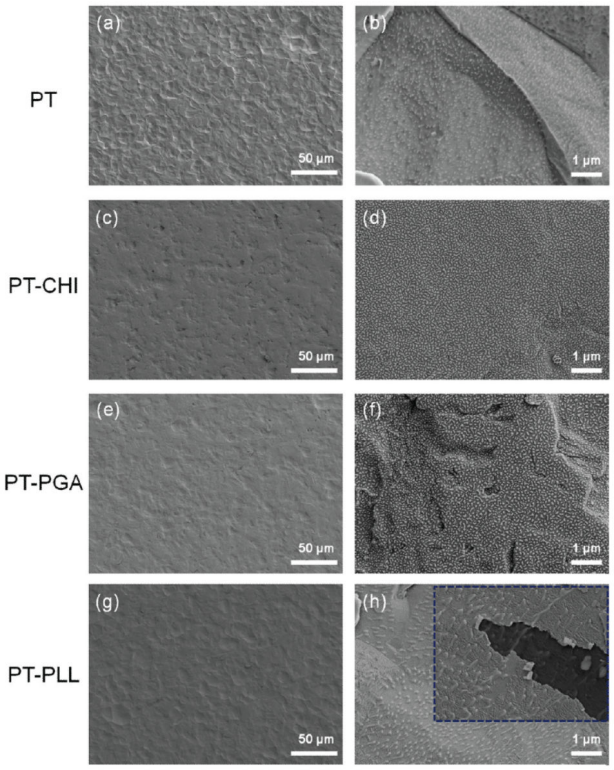

Figure 4.

SEM surface morphology images of PT surfaces after polyelectrolyte coating: PT control, PT-CHI, PT-PGA, and PT-PLL. The left column (a, c, e, g) of each image shows the surface features in lower magnification and the right column (b, d, f, h) of each image shows the surface features in higher magnification.

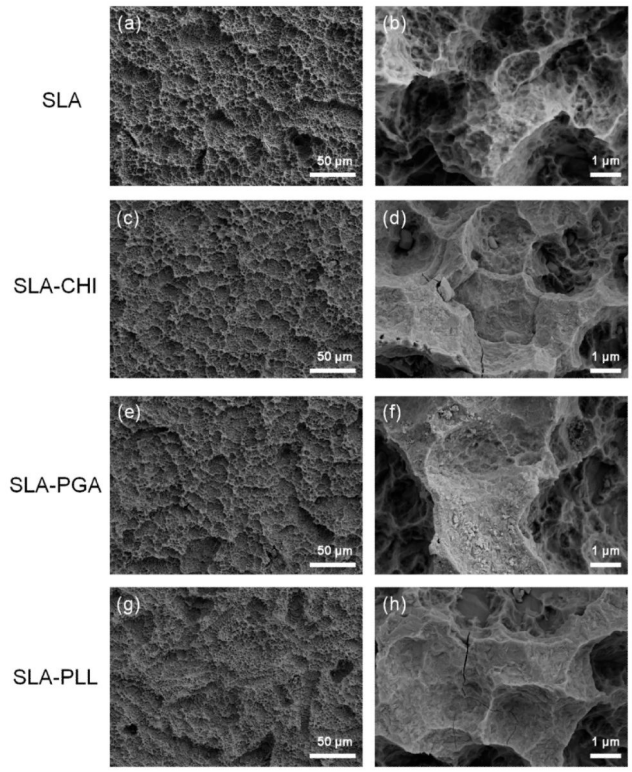

Figure 5.
SEM surface morphology images of SLA surfaces after polyelectrolyte coating: SLA control, SLA-CHI, SLA-PGA, and SLA-PLL. The left column (a, c, e, g) of each image shows the surface features in lower magnification, and the right column (b, d, f, h) of each image shows the surface features in higher magnification.

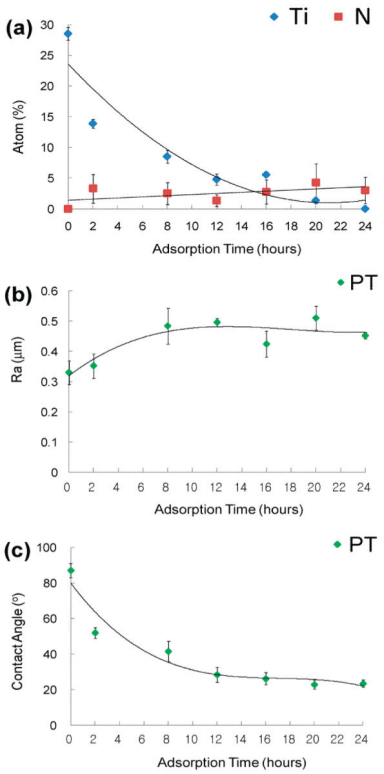

Figure 6.

Influence of the CHI adsorption time on (a) XPS atom (%) analysis for Ti vs N, (b) roughness, and (c) contact angle on PT surfaces, respectively.

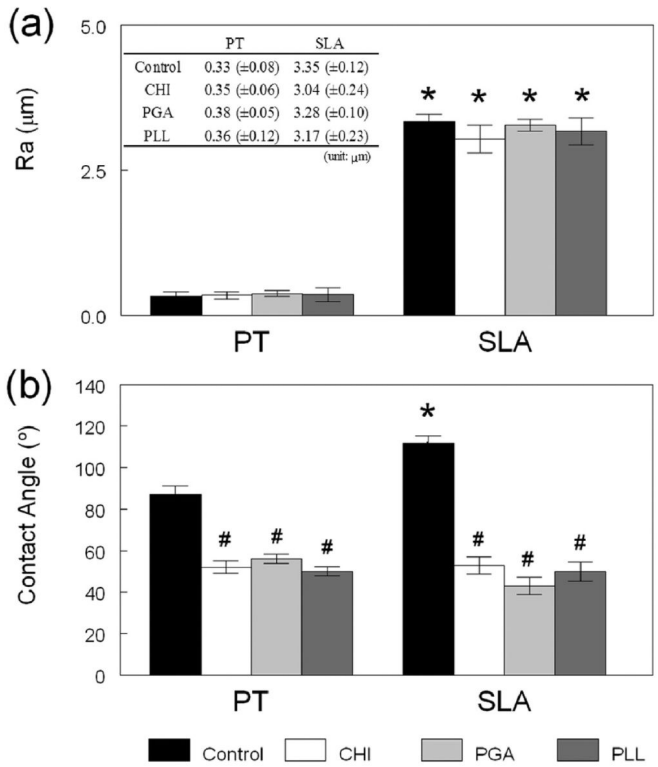

Figure 7.

Influence of the polyelectrolyte coating on (a) roughness and (b) contact angle on PT and SLA surfaces, respectively. *$p < 0.05$, PT vs SLA surface; #$p < 0.05$, polyelectrolyte coated surfaces vs control surface. The table in part a shows the actual surface roughness measurements and the associated experimental errors. The ~0.3 μm average surface roughness values of the PT and coated PT surfaces correspond to the images in Figure 4, and the ~3 μm average surface roughness values of the SLA and coated SLA surfaces correspond to the images in Figure 5.